Modelling phytoplankton succession on the Bering Sea shelf: role of climate influences and trophic interactions in generating *Emiliania huxleyi* blooms 1997–2000

Agostino Merico[a,*], Toby Tyrrell[a], Evelyn J. Lessard[b], Temel Oguz[c], Phyllis J. Stabeno[d], Stephan I. Zeeman[e], Terry E. Whitledge[f]

[a]*School of Ocean and Earth Science, Southampton Oceanography Centre, European Way, Southampton SO14 3ZH, UK*
[b]*School of Oceanography, University of Washington, Seattle, WA 98195, USA*
[c]*Institute of Marine Sciences, Middle East Technical University, Erdemli, Turkey*
[d]*Pacific Marine Environmental Laboratory, NOAA, 7600 Sand Point Way NE, Seattle, WA 98115, USA*
[e]*University of New England, 11 Hills Beach Road, Biddeford, ME 04005, USA*
[f]*Institute of Marine Science, University of Alaska Fairbanks, Fairbanks, AK 99775, USA*

Abstract

Several years of continuous physical and biological anomalies have been affecting the Bering Sea shelf ecosystem starting from 1997. Such anomalies reached their peak in a striking visual phenomenon: the first appearance in the area of bright waters caused by massive blooms of the coccolithophore *Emiliania huxleyi* (*E. huxleyi*). This study is intended to provide an insight into the mechanisms of phytoplankton succession in the south-eastern part of the shelf during such years and addresses the causes of *E. huxleyi* success by means of a 2-layer ecosystem model, field data and satellite-derived information. A number of potential hypotheses are delineated based on observations conducted in the area and on previous knowledge of *E. huxleyi* general ecology. Some of these hypotheses are then considered as causative factors and explored with the model. The unusual climatic conditions of 1997 resulted most notably in a particularly shallow mixed layer depth and high sea surface temperature (about 4 °C above climatological mean). Despite the fact that the model could not reproduce for *E. huxleyi* a clear non-bloom to bloom transition (pre- vs. post-1997), several tests suggest that this species was favoured by the shallow mixed layer depth in conjunction with a lack of photoinhibition. A top-down control by microzooplankton selectively grazing phytoplankton other than *E. huxleyi* appears to be responsible for the long persistence of the blooms. Interestingly, observations reveal that the high N:P

---

*Corresponding author. Tel.: +44-23-80593638; fax: +44-23-80593052.
E-mail address: a.merico@soc.soton.ac.uk (A. Merico).

ratio hypothesis, regarded as crucial in the formation of blooms of this species in previous studies, does not hold on the Bering Sea shelf.

1. Introduction

The Bering Sea (the eastern part being shown in Fig. 1) is divided almost equally in areal extent between a deep basin (maximum depth 3500 m) and the continental shelf (with depths less than 200 m). Three hydrographic domains (Coachman, 1986) can be identified over the shelf (coastal, middle and outer). The domains are separated by fronts, located approximately at the 50 and 100 m isobaths, and at the shelf break (150–200 m). The characteristic of the water columns at these three domains are very different. Typically, tides and
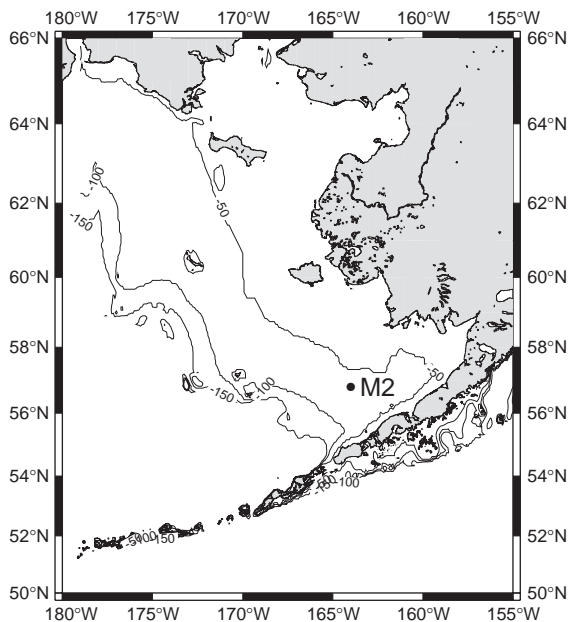

Fig. 1. Map of the eastern Bering Sea with bathymetric contour lines indicating the three hydrographic domains: (1) the coastal domain from the coast line to the 50 m isobath; (2) the middle domain from the 50 m isobath to the 100 m isobath; and (3) the outer domain approximately between the 100 and 150 m isobaths. M2, at 56.8°N 164°W, marks mooring station 2 around which the current model is applied.

winds keep all the water in the coastal domain fairly mixed throughout the year. Solar heating in the warmer seasons stratifies the middle domain waters into two strongly isolated layers, the upper being mixed by winds and the lower being mixed by tides. The outer domain waters have a more complex structure due to the vertical and horizontal currents along the shelf break.

The Bering Sea continental shelf is one of the most productive regions of the world (Walsh et al., 1989). However, its ecosystem has undergone significant disruptions, which have been most evident after the mid 1990s (Stabeno et al., 2001). The changes in the Bering Sea seem to be linked to a series of climate-induced anomalies (Overland et al., 2001). According to observations, sea surface temperature (SST) was unusually warmer in 1997 as a result of atmospheric oscillations that combined to create reduced cloud cover and therefore increased irradiance at the water surface (Overland et al., 2001; Stabeno et al., 2001).

The climatic anomalies were accompanied by several disruptions of the biotic components of the ecosystem (Stockwell et al., 2001; Baduini et al., 2001; Brodeur et al., 2002) including a massive bloom of the coccolithophore *Emiliania huxleyi* (Vance et al., 1998; Sukhanova and Flint, 1998). Blooms of this species and of such magnitude have never been observed in this area before 1997. However, a recent satellite study (Merico et al., 2003) found that a small bloom was already present in 1996. Field measurements in the early 1990s also provide evidence that *E. huxleyi* was present in the Bering Sea before 1997 (M. V. Flint, personal communication), although at concentrations lower than $1000 \text{ cells ml}^{-1}$. Typically, the blooms (or the white waters associated with them) appeared between late June and early August every year from 1997 and lasted up to October (Sukhanova and Flint, 1998; Broerse et al., 2003).

They seem to have disappeared since 2001 (Broerse et al., 2003).

E. huxleyi has been recognised as an extremely cosmopolitan species (Winter et al., 1994), although it only reaches bloom concentrations ($>1000\,\text{cells}\,\text{ml}^{-1}$) in a few areas, most notably the subarctic North Atlantic and adjacent seas. In this respect the case of the Bering Sea stands out even more as an unusual phenomenon. Among all the coccolithophores, *E. huxleyi* is the most abundant species. It is the only coccolithophore that over-calcifies, that is to say the only one which produces a quantity of calcium carbonate plates (the coccoliths) higher than the number that the cell can actually hold ($10–50\,\text{coccoliths}\,\text{cell}^{-1}$, Balch et al., 1993). This excess of coccoliths is therefore shed into the surrounding waters and, because of their property of backscattering light, the blooms are easily detectable by satellites.

Notwithstanding the importance of the specific consequences that the unprecedented massive *E. huxleyi* presence might have had on the Bering Sea ecosystem, such blooms have also global significance. Environmental impact through dimethyl-sulphide production, large fluxes of calcium carbonate being exported out of the surface waters and changes in the CO_2 air–sea fluxes have all been associated with these blooms (Westbroek et al., 1993).

In this study, a phytoplankton competition model has been developed and used in conjunction with field and satellite data. The intention is to use this tool in order to investigate how *E. huxleyi* might have become the dominant species of the summer assemblages of the Bering Sea in the period from 1997 to 2000. In particular, the potential relative roles of: (1) reduced vertical exchange, (2) photoinhibition, (3) zooplankton selective grazing, (4) effect of coccoliths, and (5) N:P ratio are considered for the formation and duration of *E. huxleyi* blooms.

The hypotheses outlined above are derived both from the typical conditions found in the past to play an important role in *E. huxleyi* bloom formation, and also from field observations in the Bering Sea. However, not all of them have been considered as causative factors and investigated with the current model. The motivations for considering or discounting a certain hypothesis are briefly presented in the following section. The way the considered hypotheses are incorporated into the model is illustrated in Section 3. Their mutual effect, explored with sensitivity analyses, is presented in Section 4 and discussed in Section 5.

2. Working hypotheses

2.1. Reduced vertical exchange

A reduced vertical exchange in 1997, because of sunnier weather (Fig. 2) and weaker winds (Stabeno et al., 2001), might have given a competitive advantage to *E. huxleyi*. This is based on the observation that, once depleted with nutrients, stratified waters may be a good environment for *E. huxleyi* (Brand, 1994). In particular, waters with very low silicate concentrations ($<2\,\mu\text{M}$) are thought to represent a favourable environment for this species when in competition with diatoms (Egge and Aksnes, 1992). Temperature distributions (Fig. 2) show a higher gradient of temperature during the summer periods between the upper mixed layer and bottom waters in 1997 (about $12\,^\circ\text{C}$) as compared to other years (between 7 and $8\,^\circ\text{C}$). According to these data, the temperature gradient in 1997 is about 1.5 times higher than other years. A stronger stratification in 1997, as a consequence of weaker winds (Stabeno et al., 2001), might have acted as a barrier for vertical advection of nutrients allowing *E. huxleyi* to establish a very high population. This hypothesis has been investigated.

2.2. Photoinhibition

Several authors have studied the effect of light saturation and inhibition on phytoplankton (Platt et al., 1980; Kirk, 1994). It appears from these studies that photosynthesis saturates in diatoms at levels of irradiance of about $120\,\text{W}\,\text{m}^{-2}$, with a rather drastic decline of the photosynthetic rate at higher light intensities. For example, a reduction to only 20% of the maximum photosynthetic rate is observed in natural diatom assemblages at $360\,\text{W}\,\text{m}^{-2}$ (Kirk, 1994, see Fig. 10.1). Nanninga
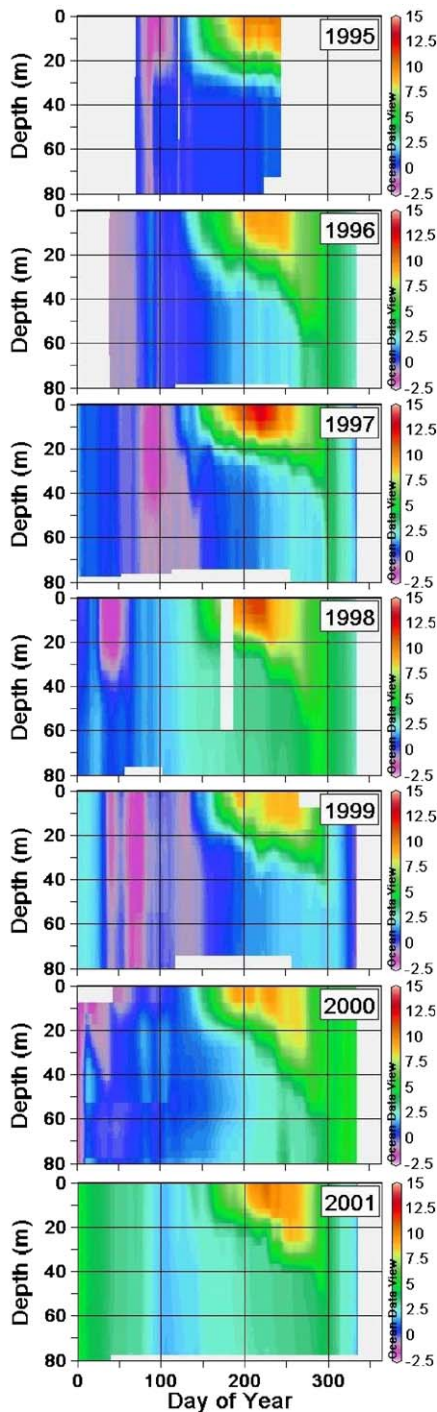
Fig. 2. Temperature distribution with depth and time in the Bering Sea at mooring station 2. Dark blue areas indicate temperatures of approximately $-1.7\,^{\circ}$C, which occur when ice is over the mooring site. Plot created using Ocean Data View 2002 software by R. Schlitzer (http://www.awi-bremerhaven.de/GEO/ODV).

and Tyrrell (1996) measured the light saturation level for *E. huxleyi* and noticed a slight photoinhibiting effect (reduction to between 80% and 95% of maximum rate) only at very high light values (between 240 and 360 W m^{-2}). In the Bering Sea, moreover, photoinhibition has been indicated in the past as a factor that could affect the spring bloom (Eslinger and Iverson, 2001). On the basis of these observations, it can be expected that the unusually clear sky conditions of the Bering Sea in 1997 might have created a favourable niche for *E. huxleyi*. Such a possibility has been investigated in this study.

2.3. Microzooplankton grazing

There is a growing body of evidence in oligotrophic regions (Lessard and Murrell, 1998) but also in eutrophic areas (Strom et al., 2001) that microzooplankton (i.e. protists and metazoan, sizes $<200\,\mu$m) can be the dominant consumers of phytoplankton production, capable of consuming more than 100% of daily primary production (Verity and Smetacek, 1996). Although some previous studies have indicated that *E. huxleyi* was readily grazed by microzooplankton (Holligan et al., 1993; Levasseur et al., 1996), others have found reduced grazing by microzooplankton on *E. huxleyi*. Based on pigment analyses in dilution experiments, Fileman et al. (2002) observed that photosynthetic dinoflagellates rather than *E. huxleyi* were selectively grazed within an *E. huxleyi* bloom off the Devon (UK) coast. Low microzooplankton grazing on *E. huxleyi* cells relative to total chlorophyll was also found in a bloom in the North Sea (Archer et al., 2001). In the Bering Sea, within the *E. huxleyi* bloom in 1999, Olson and Strom (2002) found that microzooplankton selectively grazed phytoplankton $>10\,\mu$m (i.e. larger than *E. huxleyi*), but this differential grazing was not found outside bloom waters. That selective grazing might have favoured *E. huxleyi* in proliferating and in maintaining high abundances for a relatively long time, has been investigated.

2.4. Effect of coccoliths

In a recent study, Tyrrell et al. (1999) found that coccoliths cause the surface waters to become

brighter (more irradiance available in the top few metres due to the fact that coccoliths scatter light rather than absorbing it) and the deeper waters to become darker. According to this finding, in the current model of the upper mixed layer ecosystem in which there is no phytoplankton activity in the bottom box (see Section 3), it is assumed that coccoliths will not increase the extinction of light in the (relatively shallow) upper box. In any case, given that coccoliths are shed during the senescent phase of the bloom, they will not have any impact on the establishment of the bloom. Therefore, the processes of production and shedding of coccoliths are simulated in this study only in order to compare them with the duration of the bright waters detected by the satellite.

2.5. N:P ratio

High N:P ratio has been suggested as crucial for *E. huxleyi* success in the past, either by modelling studies forced with field (Tyrrell and Taylor, 1996) and mesocosm data (Aksnes et al., 1994), and by culture experiments (Riegman et al., 2000). This hypothesis is based on the observation that *E. huxleyi* has a high affinity for inorganic phosphate and on its high ability to express a strong alkaline phosphatase activity, which makes this species able to access phosphorus contained in organic matter. From a compilation of data (Fig. 3), it has become clear that inorganic phosphate is never more limiting than inorganic nitrate in the Bering Sea, neither before 1996, when *E. huxleyi* was not present in the area in blooming concentrations, nor after, when the massive blooms took place. These data suggest that alkaline phosphatase activity by *E. huxleyi* did not play any role for its success in the Bering Sea, therefore this hypothesis has not been considered as a causative factor.

In summary, the hypotheses that will be considered as causative factors and implemented into the model are: (1) reduced vertical exchange, (2) photoinhibition and (3) zooplankton selective grazing.

3. Model description

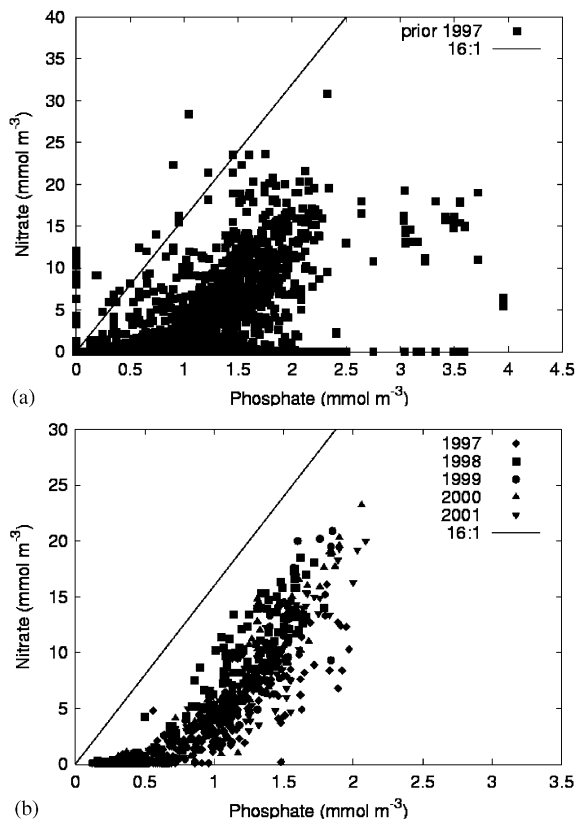The models of Aksnes et al. (1994) and Tyrrell and Taylor (1996) are the only ones in the

Fig. 3. N:P ratios in the whole water column of the Bering Sea shelf (a) before 1997 (*E. huxleyi* not present) and (b) after 1997 (*E. huxleyi* present). Data source (a) World Ocean Database 1998 and (b) T/V Oshoro Maru public reports (Anonymous, 2002). The 16:1 line represents the Redfield ratio.

literature that include *E. huxleyi* explicitly as an extra state variable of the ecosystem. These two models together with the one of Fasham (1995) provided the basic structure for the ecosystem model presented here.

The complete list of model equations can be found in Appendix A. The lists of parameters and variables used are given in Tables 1 and 2. Below, the physical aspects of the model are described, together with the structure of the ecosystem and the key factors that characterise *E. huxleyi*.

3.1. Physical aspects

In common with Tyrrell and Taylor (1996), a simple 2-layer physical structure has been adopted.

Table 1
Parameters used in the model for baseline and standard runs. References for these values are given in the text

Parameter	Symbol	Unit	Value
Diatoms (P_d)			
Maximum growth rate at $0\,^\circ$C	$\mu_{0,d}$	d^{-1}	1.2
Minimum sinking speed	v_d	m d^{-1}	0.5
Mortality rate	m_d	d^{-1}	0.08
Light saturation constant	$I_{s,d}$	W m^{-2}	15
Nitrate half-saturation constant	$N_{h,d}$	mmol m^{-3}	1.5
Ammonium half-saturation constant	$A_{h,d}$	mmol m^{-3}	0.05
Silicate half-saturation constant	S_h	mmol m^{-3}	3.5
Flagellates (P_f)			
Maximum growth rate at $0\,^\circ$C	$\mu_{0,f}$	d^{-1}	0.65
Mortality rate	m_f	d^{-1}	0.08
Light saturation constant	$I_{s,f}$	W m^{-2}	15
Nitrate half-saturation constant	$N_{h,f}$	mmol m^{-3}	1.5
Ammonium half-saturation constant	$A_{h,f}$	mmol m^{-3}	0.05
Dinoflagellates (P_{df})			
Maximum growth rate at $0\,^\circ$C	$\mu_{0,df}$	d^{-1}	0.6
Mortality rate	m_{df}	d^{-1}	0.08
Light saturation constant	$I_{s,df}$	W m^{-2}	15
Nitrate half-saturation constant	$N_{h,df}$	mmol m^{-3}	1.5
Ammonium half-saturation constant	$A_{h,df}$	mmol m^{-3}	0.05
E. huxleyi (P_{eh})			
Maximum growth rate at $0\,^\circ$C	$\mu_{0,eh}$	d^{-1}	1.15
Mortality rate	m_{eh}	d^{-1}	0.08
Light saturation constant	$I_{s,eh}$	W m^{-2}	45
Nitrate half-saturation constant	$N_{h,eh}$	mmol m^{-3}	1.5
Ammonium half-saturation constant	$A_{h,eh}$	mmol m^{-3}	0.05
Nitrate (N)			
Deep concentration	N_0	mmol m^{-3}	20
Nitrification rate	Ω	d^{-1}	0.05
Silicate (S)			
Deep concentration	S_0	mmol m^{-3}	35
Microzooplankton (Z_{mi})			
Assimilation efficiency (silicate $<3\,\mu$M)	$B_{eh,mi}, B_{f,mi}, B_{d,mi}$	—	0.75, 0.75, 0.75
Assimilation efficiency (silicate $>3\,\mu$M)	$B_{eh,mi}, B_{f,mi}, B_{d,mi}$	—	0.75, 0.75, 0.0
Grazing preferences (silicate $<3\,\mu$M)	p_{eh}, p_f, p_d	—	0.33, 0.33, 0.33
Grazing preferences (silicate $>3\,\mu$M)	$p_{eh,mi}, p_{f,mi}, p_{d,mi}$	—	0.5, 0.5, 0.0
Max. ingestion rates (baseline run)	$g_{f,mi}, g_{d,mi}$	d^{-1}	0.7, 0.175
Max. ingestion rates (silicate $<3\,\mu$M)	$g_{eh,mi}, g_{f,mi}, g_{d,mi}$	d^{-1}	0.175, 0.7, 0.7
Max. ingestion rates (silicate $>3\,\mu$M)	$g_{eh,mi}, g_{f,mi}, g_{d,mi}$	d^{-1}	0.7, 0.7, 0.0
Grazing half-saturation constant	$Z_{h,mi}$	mmol m^{-3}	1.0
Mortality rate	m_{mi}	d^{-1}(mmol m^{-3})$^{-1}$	0.05
Excretion rate	e_{mi}	d^{-1}	0.025
Fract. of mort. going into ammonium	δ_{mi}	—	0.1

Table 1 (*continued*)

Parameter	Symbol	Unit	Value
Mesozooplankton (Z_{me})			
Assimilation efficiency	$B_{d,me}, B_{mi,me}, B_{df,me}$	—	0.75, 0.75, 0.75
Grazing preferences	$p_{d,me}, p_{mi,me}, p_{df,me}$	—	0.33, 0.33, 0.33
Max. ingestion rates	$g_{d,me}, g_{mi,me}, g_{df,me}$	d^{-1}	0.7, 0.7, 0.7
Grazing half-saturation constant	$Z_{h,me}$	$mmol\,m^{-3}$	1.0
Mortality rate	m_{me}	$d^{-1}(mmol\,m^{-3})^{-1}$	0.2
Excretion rate	e	d^{-1}	0.1
Fract. of mort. going into ammonium	δ_{me}	—	0.1
Detritus (D)			
Sinking speed	v_D	$m\,d^{-1}$	1.0
Breakdown rate	m_D	d^{-1}	0.05
Cross-thermocline mixing rate	k	$m\,d^{-1}$	0.01

Table 2
Parameters used to model the calcification process. References for these values are given in the text

Parameter	Symbol	Unit	Value
Attached coccoliths (L_a)			
Calcification rate	C_{max}	$mg\,cal\,C\,(mg\,org\,C)^{-1}\,d^{-1}$	0.2
Light half-saturation constant	I_h	$W\,m^{-2}$	40
Max. number of coccoliths on a cell	Π_{max}	$coccoliths\,cell^{-1}$	30
Rate of detachment	γ	d^{-1}	24.0
Calcite C content of a coccolith	C_L	$g\,cal\,C\,coccolith^{-1}$	0.25×10^{-12}
Organic C content of an *E. huxleyi* cell	C_{eh}	$g\,org\,C\,cell^{-1}$	10.0×10^{-12}
C:N ratio	ρ_{CN}	—	6.625
Free coccoliths (L_f)			
Dissolution rate	Θ	d^{-1}	0.05
Fraction of grazed free coccoliths	δ_f	—	0.5

This does not include lateral advection effects on phytoplankton succession. Such approximation is reasonable when considering that long-term average current speeds within the Bering Sea middle shelf domain are low (on the order of $1\,cm\,s^{-1}$, Coachman, 1986). Blooms of *E. huxleyi* are usually found in stabilised and well stratified waters (Nanninga and Tyrrell, 1996). In the Bering Sea the blooms took place predominantly in the middle shelf domain (as shown in Fig. 4) where the water column is typically stratified into two layers during the warm seasons (see Fig. 2) and where tides have no direct effect on the upper box (see Section 1). The model is intended to represent the southern part of the middle shelf region around station M2 (Fig. 1). The water column is therefore simulated with two boxes. The biological activity takes place only in the upper box. The lower box represents the nutrient pool with nutrient concentrations kept constant throughout the year (N_0 and S_0 for nitrate and silicate, respectively). Nutrients are supplied to the upper box by two
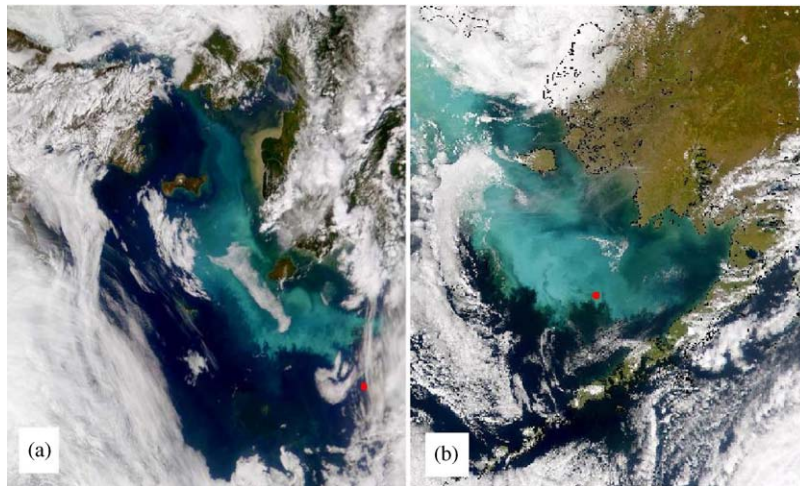
Fig. 4. (a) *E. huxleyi* bloom in the Bering Sea on 20 July 1998 and (b) 16 September 2000. Images show areas of different size. The red dots mark the location of station M2. Note how the bright water patches stretch along the middle shelf domain (compare with Fig. 1). Images provided by the SeaWiFS Project, NASA/Goddard Space Flight Center, and ORBIMAGE.

processes: entrainment and diffusive mixing across the interface (see for example Fasham, 1993). Diffusive mixing is parameterised by means of a constant factor, k.

The model is forced with variable photosynthetic active radiation (PAR) by using 6-hourly climatology data from the European Centre for Medium-Range Weather Forecast (ECMWF). PAR attenuation through depth is then simulated using the attenuation model of Anderson (1993). A variable mixed layer depth (MLD) is also used to force the model. MLD has been reconstructed from mooring temperature (T) data (Fig. 2) as the depth at which T differs by $0.5\,°C$ from its sea surface value (SST). SST is also used to control phytoplankton growth through Eppley's formulation (Eppley, 1972). Note that a recent modelling paper (Moisan et al., 2002) suggests that this formulation is inadequate to represent phytoplankton growth. The same paper presents an alternative temperature relationship which is yet to be tested in other models. Given this uncertainty in the temperature dependency of biological processes, it was decided to use Eppley's function, in common with other studies (Sarmiento et al., 1993; Doney et al., 1996). Seasonal variations of noon PAR, MLD and SST from 1995 to 2002 are shown in Fig. 5.

3.2. Food web structure

The compartments (i.e. state variables) to include into the ecosystem have been chosen according to the aim of this study which is the understanding of the factors that contributed to the seasonal succession of the most common phytoplankton groups of the Bering Sea observed during 1995–2001. The necessity to have sufficient complexity, in order to produce simulations that compare well with observation, but avoiding an excessive number of parameters has also shaped the model. The food web structure (Fig. 6) takes into account 3 typical phytoplankton groups of the region (Sukhanova et al., 1999): diatoms (P_{d}), flagellates (P_{f}) and dinoflagellates (P_{df}), as well as the species *E. huxleyi* (P_{eh}). Three main nutrients are considered: silicate (S), nitrate (N) and ammonium (A), with silicate used only by diatoms. Two different classes of zooplankton are included: microzooplankton (Z_{mi}) and mesozooplankton (Z_{me}). Diatoms, dinoflagellates and microzooplankton are the food sources for mesozooplankton, flagellates and *E. huxleyi* are the food sources for microzooplankton. Under certain conditions (see below), microzooplankton can also graze on diatoms. The problem of how to realistically
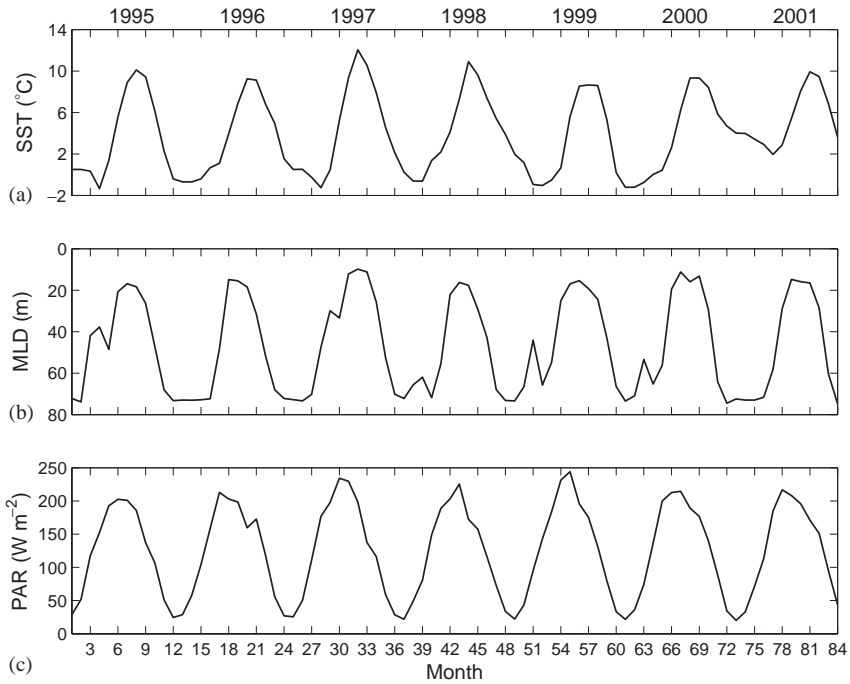
Fig. 5. Monthly running averages of: (a) sea surface temperature, (b) Mixed layer depth and (c) photosynthetically active radiation at noon. Note that the ecosystem model is actually forced with hourly values.
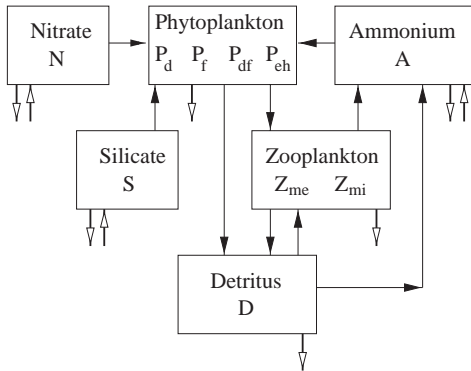

Fig. 6. Simplified foodweb used to simulate the lower trophic levels of the ecosystem in Bering Sea middle shelf area. Open arrows indicate exchanges of material between compartments and waters of the bottom box. Silicate is require by diatoms only.

simulate the remineralisation of zooplankton faecal pellets and dead plankton into ammonium has been tackled by including a detrital compartment (D) with a fixed sinking rate. The breakdown

of detritus to ammonium is also represented. In order to reduce complexity, the role of bacteria as a mediator of this process has not been included, following Fasham (1995). Coccoliths are included in the model as attached (i.e. part of the coccosphere) and free coccoliths (i.e. those which have become detached from the coccosphere), L_a and L_f, respectively. Their modelling is discussed in more detail in Section 3.4.

3.3. E. huxleyi advantages

An extra grazing term is included in the diatom equation ($G_{d,mi}P_d$ in Eq. (A.8)) to simulate the effect of microzooplankton selectively switching from *E. huxleyi* or other flagellates to diatoms (Olson and Strom, 2002). This term is introduced when silicate concentrations fall below the threshold of $3\,\mu M$. When this is the case, the maximum ingestion rate of diatoms (see Eq. (A.12)), $g_{d,mi}$, is "switched" from 0 to $0.7\,d^{-1}$ and the one of *E. huxleyi*, $g_{eh,mi}$, from 0.7 to $0.175\,d^{-1}$. This

scenario has its ecological foundation in the fact that when waters are depleted with silicate, diatoms frustules are more weakly silicified (Ragueneau et al., 2000; Goering and Iverson, 1981, observed in the Bering Sea) and this may increase their susceptibility to grazing. The reduction in grazing on *E. huxleyi* is based on evidence from field studies (e.g. Olson and Strom, 2002) as well as laboratory studies that have shown the use of chemical defenses by this species (Strom et al., 2003). The underlying assumption here is that the newly arrived *E. huxleyi* in the Bering Sea represent a sub-optimal prey for microzooplankton as compared to the lightly silicified summer diatom population.

Photoinhibition is incorporated in the current model by calculating light-limited growth using a Steele's function (Eq. (A.3)). The growth of *E. huxleyi* is assumed to saturate at higher irradiances than for all other phytoplankton (see Table 1 for values). In combination with different maximum growth rates (at $0\,^\circ$C), this formulation of light limitation will give *E. huxleyi* a relative disadvantage at low light levels and a relative advantage at high light levels (see Fig. 7).

Young (1994) observed that *E. huxleyi* predominates in areas of upwelling and in coastal and shallow sea assemblages. In addition, Hurlburt (1990) classified *E. huxleyi* together with diatoms as fast growing, *r*-selected species. These indications
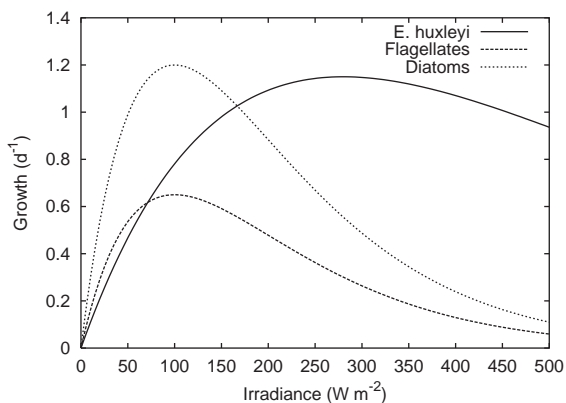
suggest a higher maximum growth rate for *E. huxleyi* with respect to other small phytoplankton such as flagellates. It was for this reason that Tyrrell and Taylor (1996) adopted a high growth rate for *E. huxleyi* in their ecosystem model, comparable to the one for diatoms but somewhat smaller. In this study, a maximum growth rate of $1.15\,\mathrm{d}^{-1}$ has been assumed for *E. huxleyi*, $1.2\,\mathrm{d}^{-1}$ for diatoms, $0.65\,\mathrm{d}^{-1}$ for flagellates and $0.6\,\mathrm{d}^{-1}$ for dinoflagellates. During the spring blooms of the years 1980 and 1981 a maximum growth rate of about $1.2\,\mathrm{d}^{-1}$ was determined in the Bering Sea (Eslinger and Iverson, 2001).

3.4. Other major processes and parameters

Half-saturation constants for phytoplankton nutrient uptake are equal for all groups and species and set to $1.5\,\mathrm{mmol\,m^{-3}}$ for nitrate uptake (which is within the range of 0.5–$2.75\,\mathrm{mmol\,m^{-3}}$ determined by Sambroto et al. (1986) in the Bering Sea) and $0.05\,\mathrm{mmol\,m^{-3}}$ for ammonium uptake (Tyrrell and Taylor, 1996). Phytoplankton natural mortality is modelled linearly with a constant rate set to $0.08\,\mathrm{d}^{-1}$ for all groups and species (slightly higher than $0.05\,\mathrm{d}^{-1}$ used by Fasham, 1995). Among phytoplankton only diatoms are assumed to sink. Sinking takes place at a minimum velocity of $0.5\,\mathrm{m\,d^{-1}}$, as silicate becomes depleted ($<2\,\mu\mathrm{M}$) this velocity is increased as described by Tyrrell and Taylor (1996). The grazing processes have been simulated with an Holling type III function as in Fasham et al. (1990). Zooplankton losses are by excretion (directly remineralised into ammonium) and mortality (of which 10% is remineralised directly into ammonium and the rest is assumed to sink rapidly out of the system). Detritus is lost out of the system by sinking (at a constant rate of $1\,\mathrm{m\,d^{-1}}$) and remineralised into ammonium through a constant breakdown rate of 5% per day.

The "bright water" signal produced by the coccoliths and detected by satellites can give useful information on the duration of *E. huxleyi* blooms. In order to compare this signal with the duration of the blooms predicted by the model, the seasonal cycles of attached and free coccoliths are simulated. Since the details of how and why the

Fig. 7. Comparison of *PI*-curves for *E. huxleyi*, flagellates and diatoms in the model. Saturation level is set to $280\,\mathrm{W\,m^{-2}}$ for *E. huxleyi*, and to $100\,\mathrm{W\,m^{-2}}$ for all other phytoplankton and with maximum growth rates as in Table 1.

coccoliths are produced and afterward detached in nature are not fully understood, it is very difficult to give a realistic representation of this processes. The only attempt so far to model such mechanisms is represented by the study of Tyrrell and Taylor (1996). The same formulation is adopted here. The production of attached coccoliths is made proportional to *E. huxleyi* concentration. Under optimal conditions coccolith production takes place at a maximum calcification rate, C_{max}, of $0.2\,\text{mg cal C}\,(\text{mg org C})^{-1}\,\text{d}^{-1}$ (Fernández et al., 1993). The process is limited by temperature and light, not by nutrients (Paasche, 2002). Attached coccoliths are lost into the free coccolith compartment by detachment, by grazing of the whole cell and by cell natural mortality. Since one calcified cell can hold a maximum of 10–50 coccoliths (Balch et al., 1993), the detachment is calculated by comparing the concentration of attached coccoliths with the concentration of *E. huxleyi* cells. When the ratio of these two variables is greater than Π_{max} coccoliths per cell (set to 30), then the coccoliths in excess are shed and transferred into the free coccolith compartment. The grazing of attached and free coccoliths is assumed to take place at the same rate as for cells ($G_{eh,mi}$). Grazed coccoliths (attached and free) are not assimilated by zooplankton (Honjo and Roman, 1978). Based on this observation, it is assumed that ingested coccoliths are egested and lost rapidly out of the system (in the form of large aggregates and faecal pellets). There are strong indications that calcite dissolution can take place at depths well above the chemical lysocline through biologically mediated processes (Harris, 1994; Milliman et al., 1999). Therefore free coccoliths are also dissolved in the model at a constant rate of 5% per day (Tyrrell and Taylor, 1996).

Diffusive vertical exchange between the two boxes has been parameterised with a multiplicative factor. Although in a rather simplistic fashion, k does take into account those processes like breaking internal waves, convective mixing and storm events. A low value of this parameter, typically $0.01\,\text{m d}^{-1}$ (Fasham, 1993), corresponds to strong stratification and therefore less diffusive exchange between the two boxes.

The model uses nitrogen as currency and, where necessary to compare results with chlorophyll

equivalents, a Redfield C:N ratio of 6.625 for phytoplankton and 5.625 for zooplankton, with a C:Chlorophyll ratio of 50.

3.4.1. Method

The system of differential equations has been solved numerically using the fourth-order Runge–Kutta method with a time step of 1 h. A linear interpolation of ECMWF data, which are 6-hourly, is used to match the time step of the model.

In order to minimise the dependency of the model results on the initial conditions of the state-variables, the model was run repeatedly over a full seasonal cycle of the physical forcing prior to 1995. Once it developed a repeatable annual cycle, it was then run with the forcing from 1995 to 2001. Results have also been checked so as to avoid solutions with multi-year cycles.

4. Results

4.1. Model validation: baseline run

A baseline run has been provided without *E. huxleyi* in order to validate the model and explore its behaviour with respect to the seasonal succession patterns and other aspects of the ecosystem observed before the increased *E. huxleyi* activity (i.e. before 1995). Parameters for this run are reported in Table 1. The forcing function for this case (SST, MLD, PAR) are obtained as the average functions that have been affecting the ecosystem in the last 20 years (before 1995) and the results compared with multi-year composites of observations (for the variables available). The observations are obtained from the World Ocean Database 1998 (WOD98), which contains data collected only until the early 1990s. The extra grazing pressure on diatoms by microzooplankton is also taken into account in this run. The model is able to reproduce the typical nutrient seasonal cycles (Figs. 8c and d). The typical Bering Sea shelf characteristic of a pronounced diatom spring bloom (Goering and Iverson, 1981; Sukhanova et al., 1999) is also predicted by the model (Fig. 8a). The autumn diatom peak produced in the simulation is also characteristic of the area, as reported
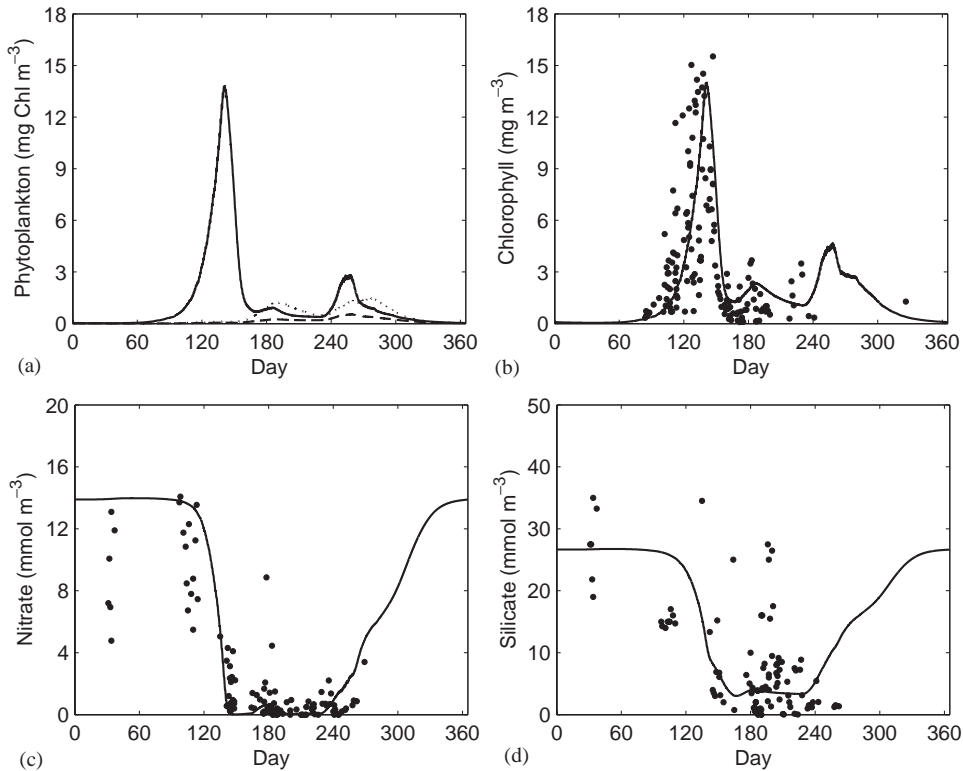
Fig. 8. Baseline run. Outputs obtained with forcing conditions prior to 1995 (*E. huxleyi* is not included in the model). The plots show: (a) modelled phytoplankton seasonal succession following the sequence of diatoms (solid line), flagellates (dotted line) and dinoflagellates (dashed line) and (b) simulated total chlorophyll, (c) nitrate and (d) silicate (continuous lines) as compared with WOD98 data (dots). See text for discussion.

by Sukhanova et al. (1999). The deepening of the MLD at the end of summer provides by entrainment nutrient resources to the best competitors in conditions of declining PAR and weakening of water column stability. Diatoms are the fastest growers in the model (and in reality). The general result of phytoplankton succession (Fig. 8a), diatoms–flagellates–dinoflagellates, is in agreement with the most common sequence observed in the area and described by Sukhanova et al. (1999). Total chlorophyll also compare well with the WOD98 data (Fig. 8b).

4.2. Standard run

The standard run (SR), i.e. the run that best fits the data available from 1995 to 2001, and give the best predictions in terms of phytoplankton

succession is presented in this section. Fig. 9a shows modelled total chlorophyll compared with SeaWiFS-derived data. All the data are compilations of observations carried out within few hundred metres from station M2 and representative of the southern middle shelf domain. The simulated seasonal succession is shown in Fig. 9b. The black horizontal bar represent periods when *E. huxleyi* blooms were seen in satellite images. This information has been obtained from the duration of bright waters seen in monthly composites of SeaWiFS true colour images (Broerse et al., 2003). Bright *winter* waters are not shown as black bars because they are not *E. huxleyi* blooms (see Broerse et al., 2003). The concentration of free coccoliths in the model follows that of *E. huxleyi*, but with a slight time lag (Fig. 9c). Nitrate and silicate seasonal cycles are reported in Figs. 9d and
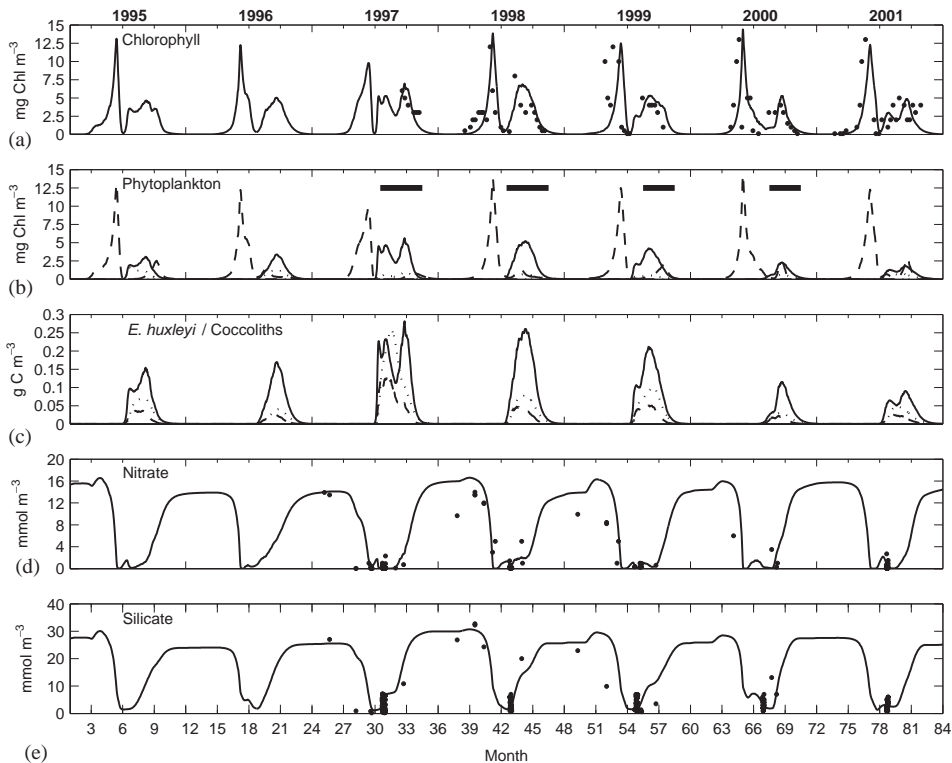
Fig. 9. Standard run 1995–2001. (a) Modelled total chlorophyll (solid line) as compared with SeaWiFS-derived chlorophyll (symbol); (b) phytoplankton succession with diatoms represented by dashed line, *E. huxleyi* by solid line and flagellates by dotted line, and with horizontal bar indicating the duration of *E. huxleyi* blooms as observed in SeaWiFS true-colour images; (c) Simulated concentrations of: *E. huxleyi* (solid line), attached coccoliths (dashed line) and free coccoliths (dotted line), (d) modelled nitrate cycles (solid line) as compared with data (symbol); and (e) silicate cycles (solid line) as compared with data (symbol).

e, respectively. The nutrient measurements are obtained in this case from Hokkaido University, T/V Oshoro Maru public data (because WOD98 contains data collected only until the early 1990s), which are published in annual reports (Anonymous, 2002) and by several cruises conducted in the area in the context of the following projects: Southeast Bering Carrying Capacity, Process Studies of the Inner Shelf, Longterm Mooring Measurements in the Bering Sea and Plankton Processes.

Modelled mesozooplankton is presented in Fig. 10 as compared with biomass data. The data (preserved wet weight) have been obtained from Hokkaido University, T/V Oshoro Maru public reports (Anonymous, 2002). Over the length of the time series considered here (1995–2001), sampling

of zooplankton began in the Bering Sea in early June and ended in early August. The samples were collected with 45 cm mouth diameter NORPAC nets (with a 0.33 mm mesh) towed vertically from 150 m or near bottom to the surface at about $1 \, \text{m s}^{-1}$. Samples that data reports noted as biased by predominance of taxa with high water content (e.g. salps) or calcareous materials (i.e. coccolitho- phores) have been excluded. Wet weight has been converted into carbon units by assuming a zooplankton water content of 83% and a carbon to ash-free dry weight ratio of 0.45, which gives a carbon to wet weight relationship of 0.092. The temporal mismatch between model and observations may be a consequence of the fact that modelled mesozooplankton peaks are always a response to the diatom spring blooms. Therefore
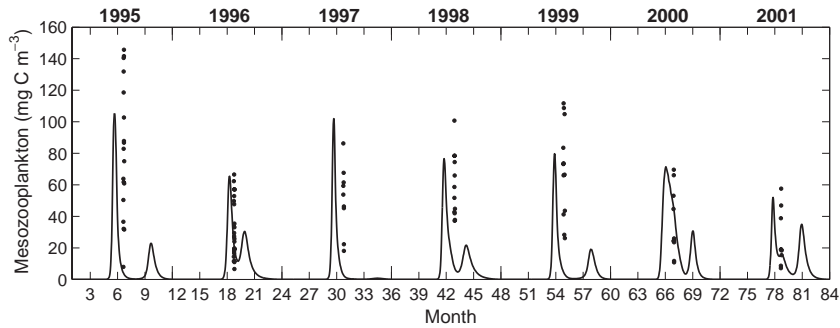
Fig. 10. Standard run 1995–2001. Modelled mesozooplankton (solid line) as compared with zooplankton biomass data (symbol). Biomass data, originally in wet weight, have been converted into carbon units by assuming a carbon to wet weight relationship of 0.092 (see text for more details).

a sampling campaign targeting the late/post spring bloom period (April–May rather than June–August) would have been more appropriate for model comparisons.

Simulated and observed phytoplankton abundance (only available for the period 1997–1999) are shown in Fig. 11. Phytoplankton samples were collected during cruises of the R/V *Alpha Helix*. Collections were made at the surface and, usually, at 5 m intervals to 40 m, preserved in neutral Lugols iodine, and kept in the dark until counted. Species were identified to lowest possible taxon, and enumerated by counting 200–400 cells per sample. Additional data points are included for *E. huxleyi* biomass (Fig. 11b, marked with triangular symbols) from: (1) values reported by Stockwell et al. (2001) relatively to September 1997 and (2) from samples of 31 July 1998 obtained on the T/V Oshoro Maru in areas of white waters. The latter were obtained by preserving the samples in buffered formalin and counted in settled samples. An additional data point is also included in the flagellates' plot (Fig. 11c, triangular symbol). This was obtained from samples of 31 July 1998 on the T/V Oshoro Maru and estimating the biomass by using actual cell sizes. In order to compare cell counts with model results (in carbon units), time-invariant carbon content of 10 pg cell^{-1} has been assumed for *E. huxleyi* (Holligan et al., 1983; Balch et al., 1992). For other groups, counts have been converted into biovolume first by assuming a mean diameter of 3 μm for flagellates

and 30 μm for diatoms. The general "protist plankton" conversion equation of Menden-Deuer and Lessard (2000) was then used for the volume to carbon conversion: $C = 0.216V^{0.939}$, where C is the carbon content per cell in pg and V is the biovolume in μm. It is worthwhile to keep in mind here that this cell number to biomass conversion is only an approximation and therefore the biomass values cannot be compared with model results in absolute terms.

The model results compare well with chlorophyll (Fig. 9a) and nutrient data (Figs. 9d and e). Note that very low *E. huxleyi* concentrations (68 cells ml^{-1}) were observed at the end of July 1998 (Fig. 11b), circular symbol. This happened because sampling was carried out just outside the bright water patch, on the spot marked by the red dot in Fig. 4a. Simulated *E. huxleyi* bloom timing and duration agree well with bright water temporal patterns observed in SeaWiFS true-colour images (represented with a black bar in Fig. 9a). A low *E. huxleyi* concentration in the years 1995 and 2001 is not however reproduced by the model. Although *E. huxleyi* cells have been found in the area since the early 1990s (see Section 1), the model does overestimate those observations. Despite this, the model gives strong suggestions on the possible causes for *E. huxleyi* arrival in the Bering Sea in 1997, as it is evident from the results of the following simple experiments. The model has been run as in the SR configuration from 1995 to 2001 but by forcing the year 1997 with functions
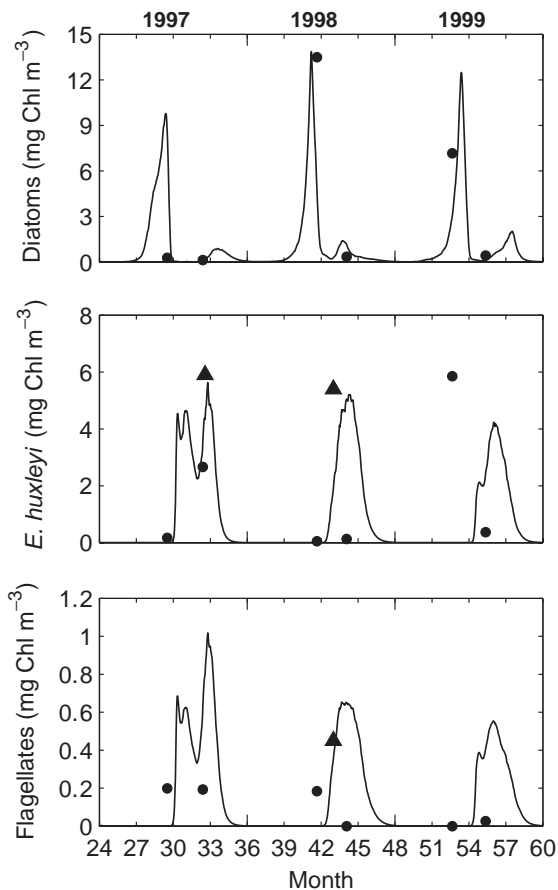
Fig. 11. Standard run 1997–1999. Modelled phytoplankton abundances (solid lines) as compared with data (symbols). More details on this comparison are given in the text. Note that in order to compare cell counts with model results (in carbon units), time-invariant carbon content has been assumed for *E. huxleyi*. For other groups, counts have been converted into biovolume first and then into carbon by using the method of Menden-Deuer and Lessard (2000).
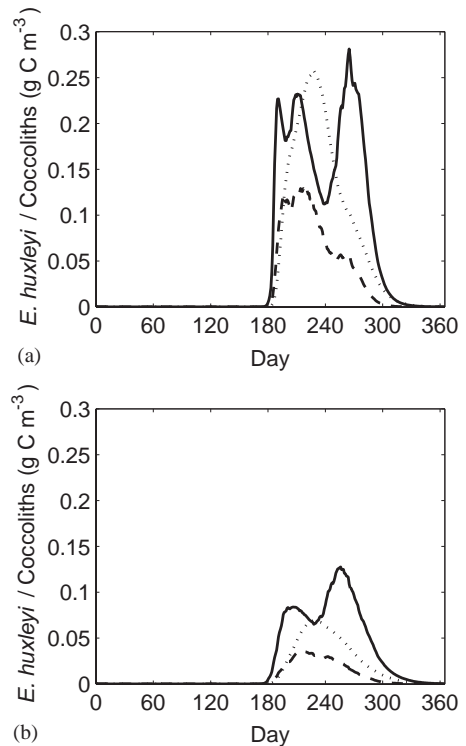

Fig. 12. Modelled concentrations of: *E. huxleyi*, attached and free coccoliths (solid, dashed and dotted lines, respectively) for the year 1997 as obtained (a) in the standard run configuration; and (b) by forcing 1997 with functions typical of a non-*E. huxleyi* year (i.e. 2001).

(SST, MLD and PAR) characteristic of 2001 (see Fig. 5), a non-*E. huxleyi* year. Fig. 12b shows the results of this experiment as compared with the SR (Fig. 12a) for the year 1997. *E. huxleyi* population and coccolith concentrations would be markedly reduced if 1997 would have been a year with physical forcings typical of a non-*E. huxleyi* year like 2001 (Fig. 12b). Furthermore, by holding one at a time out of SST, PAR and MLD at 2001 values, with the other two at 1997 values, it was

also tested the relative importance of each factor in producing the higher *E. huxleyi* concentrations in 1997. In this way it was found MLD to have the greatest impact (with a variation in the maximum population size of about 40%) and SST and PAR to have less importance (with a variation in the maximum population size of about 10%). In reality of course, all three are inter-dependent.

4.3. Sensitivity analysis

A parameter sensitivity analysis of a multi-annual multi-species plankton model presents problems of data presentation. The number of parameters to be studied would quickly lead to an unmanageable number of figures. Therefore, attention has been focused mainly on those

parameters or processes that have a direct impact on the causative factors. Runs were carried out in which individual causative factors were omitted from the model. The results of these runs were then compared with the standard run, which includes all the causative factors. In the adopted grazing formulation (see Eq. (A.12)), the grazing rate depends on the maximum ingestion rate, the food preferences and other parameters. Note, however, that the grazing hypothesis has been tested by changing only the maximum ingestion rates. This choice is supported by some extensive sensitivity studies conducted in the past (see Appendix A in Fasham et al., 1990) which have shown that the influence of the other parameters (particularly the preferences) on the grazing rate is minimal.

4.3.1. Different diffusivity regimes across the thermocline

A model sensitivity analysis of diffusive mixing (plots not shown) showed that the ecosystem experiences low vertical diffusion when k is set to $0.01 \, \mathrm{m \, d^{-1}}$ and lower, and in these cases any exchange of material between the two boxes is only driven by the dynamics of the MLD itself (see Eq. (A.1)). By increasing k, diffusive mixing becomes more and more important up to the limit of when the upper box is brought to the same nutrient concentration as in the bottom layer and with no more biological activity due to a complete loss of phytoplankton. A turbulent environment tends to favour diatoms and *E. huxleyi* due to their high maximum growth rates. However, conditions of reduced diffusive mixing in 1997 and 1998 with respect to other years did not result in the success of *E. huxleyi*, probably due to the ambiguous effect of k in supplying nutrient but also in removing plant cells (Evans, 1988).

4.3.2. No photoinhibiting effect

This condition has been implemented by assuming that all phytoplankton respond to light according to a Michaelis–Menten function (Eq. (A.4)) rather than to a Steele function (Eq. (A.3)). As in a previous study (Tyrrell and Taylor, 1996), *E. huxleyi* is assumed to have a higher half-saturation constant for light $(I_{\mathrm{h}} = 45 \, \mathrm{W \, m^{-2}})$

compared to all other groups $(I_{\mathrm{h}} = 15 \, \mathrm{W \, m^{-2}})$. The achieved growth also depends on the maximum growth rates. These parameters have been changed slightly in this run so that flagellates have an advantage at light intensities lower than approximately $70 \, \mathrm{W \, m^{-2}}$ with respect to *E. huxleyi*. This was done in order to produce *P–I* curves (shown in Fig. 13) similar to the ones obtained in the standard run configuration (Fig. 7) but now without photoinhibition. Maximum growth rates and light half-saturation constants used in this run are reported in Table 3.

This run shows that no photoinhibition will cause the flagellate population to reach the unrealistically abundances of about $5 \, \mathrm{mg \, Chl \, m^{-3}}$ (Fig. 14b), when considering that the observed concentrations, for example for the years 1997–1998, are around $0.2 \, \mathrm{mg \, Chl \, m^{-3}}$ (Fig. 11c). Note that diatoms are still under the pressure of the extra microzooplankton grazing term during summer, when silicate gets lower than $3 \, \mu\mathrm{M}$.

4.3.3. Microzooplankton not grazing on diatoms

The extra diatom loss term representing microzooplankton grazing on them ($G_{\mathrm{d,mi}} P_{\mathrm{d}}$ in Eq. (A.8)) has been omitted in this run. For this case, the maximum ingestion rate of microzooplankton feeding on *E. huxleyi* has been set to $0.7 \, \mathrm{d^{-1}}$, as for the other phytoplankton. As expected, the occurrence and magnitude of the spring bloom is not affected (see Fig. 14c). The impact is evident
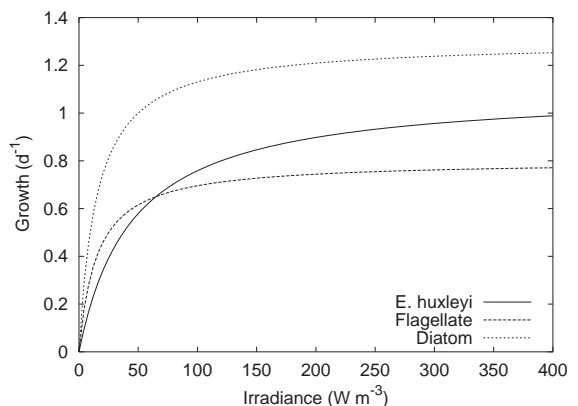

Fig. 13. Comparison of PI-curves for *E. huxleyi*, flagellates and diatoms in the case of Michaelis–Menten light-limited growth. The parameters used to simulate this scenario are given in Table 3.

between late summer and beginning of autumn when silicate is depleted. Diatoms show a somewhat higher summer peak than in the standard run but more interestingly the duration of *E. huxleyi* blooms are unrealistically reduced in this run by up to a month (compare the duration of the

blooms as inferred by SeaWiFS, horizontal bars in Fig. 14, with modelled *E. huxleyi*, blue line in Fig. 14c).

4.3.4. Microzooplankton not grazing diatoms and lightly grazing E. huxleyi

This run is similar to the previous one but this time the microzooplankton grazing pressure on *E. huxleyi* has been reduced by setting the maximum ingestion rate, $g_{eh,mi}$, to $0.175 \, d^{-1}$. Although the result (Fig. 14d) is somewhat closer to the standard run (Fig. 14a), it still remains unrealistic when compared with the observed phytoplankton abundances (Fig. 11). The 1998 *E. huxleyi* bloom disappears and the duration of the blooms after 1998 are reduced (Fig. 14d). This

Table 3
Maximum growth rates and light half-saturation constants used to explore the sensitivity of the model results in the absence of photoinhibition

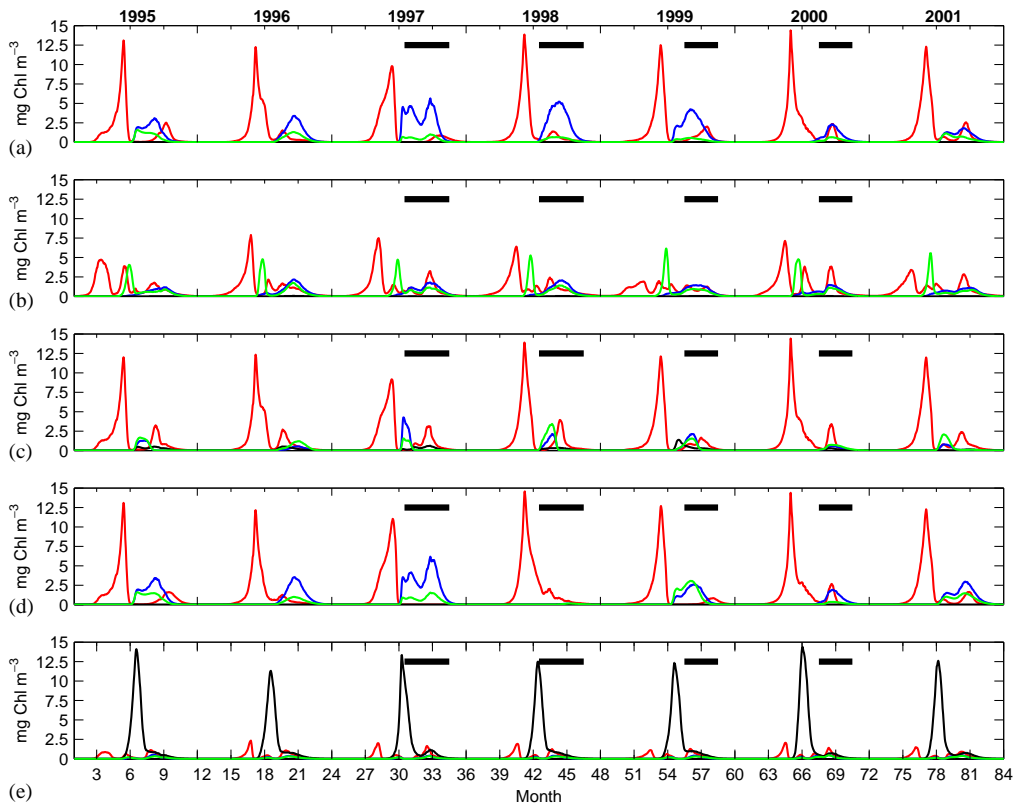|	$\mu_{max,0}$ (d^{-1})	I_h $(W\,m^{-2})$
Diatoms	1.3	15
Flagellates	0.8	15
Dinoflagellates	0.6	15
E. huxleyi	1.1	45

Fig. 14. Results of sensitivity analyses: (a) standard run, (b) no photoinhibition, (c) microzooplankton not grazing diatoms, (d) microzooplankton not grazing diatoms and only lightly grazing *E. huxleyi* and (e) microzooplankton grazing equally on diatoms, flagellates and *E. huxleyi*. In all plots the red line represents diatoms, the blue line *E. huxleyi*, the green line flagellates and the black line dinoflagellates.

run shows that a reduced grazing pressure on *E. huxleyi* without having an extra grazing pressure of microzooplankton on diatoms is not enough to explain the success of *E. huxleyi*.

4.3.5. Microzooplankton grazing equally on diatoms and E. huxleyi

This test has been carried out by putting diatoms, flagellates and *E. huxleyi* under the same microzooplankton grazing pressure. This has been realised by setting $g_{d,mi}$, $g_{f,mi}$ and $g_{eh,mi}$ all to $0.7\,d^{-1}$. Note that diatoms are still grazed by mesozooplankton with a maximum ingestion rate, $g_{d,me}$, of $0.7\,d^{-1}$. Such a scenario also leads to an unrealistic result by favouring dinoflagellates (Fig. 14e).

5. Discussion

The modelled distributions of blooms that could best reproduce the observations was obtained by assuming that *E. huxleyi* has a particular advantage at high light when photoinhibition limits the flagellates population. The model also suggests that an extra microzooplankton grazing pressure on diatoms in conjunction with a lower microzooplankton grazing pressure on *E. huxleyi* may control the bloom duration of *E. huxleyi*.

5.1. Why did E. huxleyi first bloom in the Bering Sea in 1997?

Merico et al. (2003) have shown that the intense bloom of *E. huxleyi* (concentration as high as $2.1–2.8\,10^6\,cells\,l^{-1}$) in the Bering Sea in 1997 was preceded by a small bloom in 1996. *E. huxleyi* in fact has been present in the Bering Sea at least since the early 1990s (M. V. Flint, personal communication), although not in blooming concentrations. Coccolithophores (*Pontosphaera* sp.) have also been observed in field studies carried out in the early 1970s in the Subarctic Pacific and Bering Sea (Taniguchi et al., 1976). Given these evidence, it seems plausible to assume that the Bering Sea has long been a potentially favourable place for coccolithophores. What made then *E. huxleyi* population gradually become more

active in 1996 to finally burst out in 1997 and persist until 2000? Unusual weather conditions, with persistent clear skies (Stockwell et al., 2001) were the most evident anomalous factors in 1997, which caused SST to be $4\,°C$ above the climatological mean (Stabeno et al., 2001). It has not been possible to reproduce a transition that goes from non-bloom year (1995) to small-bloom year (1996) to big-bloom years (1997–2000) with the model. However, in a simple experiment, in which forcing (SST, MLD and PAR) typical of a colder year was used in 1997, a clear reduction (about 50%) in *E. huxleyi* activity was produced (Fig. 12). In other words, particularly good weather conditions in 1997, resulting in higher SST and weaker winds, have contributed to create a shallower MLD (Fig. 5b) and to keep the water column stable for longer (Fig. 2). These conditions, in conjunction with a higher affinity for light, seem to have favoured *E. huxleyi*. It should be noted that important parameters in the model are kept constant for all the years throughout which the model is run. Undoubtedly, phytoplankton mortalities, *E. huxleyi* calcification rates, half-saturation constants for phytoplankton nutrient uptake, zooplankton maximum ingestion rates, etc. may all vary with time and location but our knowledge of their dynamical behaviour is up to now inadequate. Such a lack of information sets a limit on the model performance. Other alternative hypotheses can be identified to explain why the model did not reproduce the non-bloom to bloom transition. Changes in horizontal currents may be one of these. The winds might have played an important role in this case. However, since the model adopted here has a simple two-layer structure, such a possibility remains open.

5.2. Why was E. huxleyi successful only in the period from 1997 to 2000?

The model results suggest that at least two different processes have combined to create favourable conditions for *E. huxleyi* in the Bering Sea. A lack of photoinhibition of *E. huxleyi* appears to be important. A high maximum growth rate combined with high light saturation levels allow *E. huxleyi* to do better against flagellates.

When photoinhibition is not included, the flagellate population becomes unrealistically high. Microzooplankton selective grazing "helped" *E. huxleyi* in the competition against diatoms. This important result confirms that microzooplankton can effectively control diatom populations during summer (Olson and Strom, 2002); this was achieved in the model by assuming that grazing intensified when silicate concentrations were low ($<3\,\mu M$). This was hypothesised to be a consequence of the increased susceptibility of lightly silicified diatoms to grazing. However, it is also possible that diatoms become the most abundant preferred food in the presence of unpalatable *E. huxleyi*, and low silica conditions were simply coincidental with summer conditions. It appears that once conditions have become favourable for the establishment of a consistent seeding population (in 1997) in the Bering Sea, *E. huxleyi* had the possibility to bloom again in the following years until it faded away once climate returned to its normal state.

5.3. Why did the bloom persist for so long?

The model strongly suggests that the bloom persistence (3–4 months) is related to the microzooplankton–diatom interaction. This finding is supported by studies showing that microzooplankton are capable of choosing their prey selectively (Burkill et al., 1987) and by studies showing their ability to graze cells up to five times their own volume (Jacobson and Anderson, 1986; Hansen and Calado, 1999). The current model investigations were also based on results obtained with dilution experiments conducted in 1999 in the Bering Sea during an *E. huxleyi* bloom (Olson and Strom, 2002).

6. Conclusion

A time-dependent ecosystem model has been used in combination with field data and satellite-derived observation to clarify the phytoplankton succession stages in the Bering Sea shelf in connection with the unusual appearance of the coccolithophore *E. huxleyi*. The most likely explanation for *E. huxleyi* arrival in the Bering Sea seems to be connected to the unusual weather conditions that have been perturbing the ecosystem since 1997. The model suggests that the anomalous warm climate of 1997, resulting in higher SST, shallower MLD and higher PAR, might have played an important role in generating *E. huxleyi* blooms, under the assumption that this species is not photoinhibited by light. Another important result of this study is related to the mechanisms of succession and to *E. huxleyi* bloom duration. The unusual persistence of bright waters detected by SeaWiFS and field observations is likely to be caused by microzooplankton selectively grazing diatoms rather than *E. huxleyi*, which agrees with the general principle that selective predation can regulate the growth of certain phytoplankton at certain times of the year.

Interestingly, the important ability of *E. huxleyi* to thrive in water conditions with high N:P ratio (Riegman et al., 2000), which has been considered a crucial factor for the success of this species in the past (Aksnes et al., 1994; Tyrrell and Taylor, 1996), did not have any relevance in the Bering Sea, as revealed by observations.

The present study helps in understanding the complex interactions among phytoplankton, zooplankton and their environment in the Bering Sea while forced by unusual conditions. Nevertheless, in order to explore further the findings reported here, it is important that detailed time-series measurements of PAR and nutrients along with phytoplankton species abundance and their N- or C-content, are made so that models such as this one can be further constrained.

Appendix A. Model equations

The effect of the physical forcing (and therefore the connection with the climate) on the ecosystem is modelled implicitly by the seasonal dynamics of the mixed layer depth $M(t)$. Temperature data (as detailed functions of time and depth) have been used to reconstruct the MLD, $M(t)$. $h(t) = dM(t)/dt$ was used to calculate the time rate of change of the MLD. Exchange between the two layers was modelled as two processes, vertical turbulent diffusion and entrainment or detrainment caused by deepening or shallowing of the MLD. According to Fasham (1993), the variable $h^+(t) = \max[h(t), 0]$ was used in order to take into account the effects of entrainment and detrainment. The two zooplankton variables were considered capable of maintaining themselves within the mixed layer and thus the function $h(t)$ was used in that case. Diffusive mixing across the thermocline, k, has been parameterised by means of a constant factor. The whole diffusion term can finally be written as

$$K = \frac{k + h^+(t)}{M(t)}. \tag{A.1}$$

A.1. Phytoplankton

The phytoplankton growth rate, μ_d (for example in the case of diatoms), is a function of light,

nutrients and temperature. These terms are assumed to limit growth independently so that:

$$\mu_d = \mu_{0,d} f(T) \Psi_d(I) \Phi_d(N, A, S), \tag{A.2}$$

where $\mu_{0,d}$ is the maximum intrinsic growth rate at temperature $T = 0\,^\circ\text{C}$, $f(T) = e^{0.063T}$, and the term $\mu_{0,d} f(T)$ represents the Eppley (1972) formulation of temperature-dependent growth. The light limitation term, is calculated by integrating PAR over the depth z by using two formulations: (1) the Steele formulation (in the baseline and standard runs):

$$\Psi_d(I) = \frac{1}{M} \int_0^M \frac{I(z)}{I_{s,d}} e^{1 - I(z)/I_{s,d}} \, dz, \tag{A.3}$$

where $I_{s,d}$ is the light level at which photosynthesis saturates in the case of diatoms, and (2) the Michaelis–Menten formulation (in the sensitivity analysis run):

$$\Psi_d(I) = \frac{1}{M} \int_0^M \frac{I(z)}{I_{h,d} + I_z} \, dz, \tag{A.4}$$

where $I_{h,d}$ is the half-saturation constant of growth with respect to light. In both formulations, $I(z)$ is calculated with Anderson's model (Anderson, 1993). Following Fasham (1995), the nutrient limitation term $\Phi_d(N, A, S)$ is given by

$$\Phi_d(N, A, S) = \min\left[n_d + a_d, \frac{S}{S_h + S} \right] \tag{A.5}$$

with

$$n_d = \frac{N/N_{h,d}}{1 + N/N_{h,d} + A/A_{h,d}} \tag{A.6}$$

for nitrate limitation and

$$a_d = \frac{A/A_{h,d}}{1 + N/N_{h,d} + A/A_{h,d}} \tag{A.7}$$

for ammonium limitation. S_h, $N_{h,d}$ and $A_{h,d}$ are the half-saturation constants for diatom uptake of silicate, nitrate and ammonium, respectively. For phytoplankton other than diatoms, the limitation due to nutrient is simply given by the sum of (A.6) and (A.7).

The equations for phytoplankton can now be written as

$$\frac{dP_d}{dt} = \mu_d P_d - m_d P_d - G_{d,me} P_d$$
$$- G_{d,mi} P_d - \left(\frac{v_d}{M} + K\right) P_d, \qquad (A.8)$$

$$\frac{dP_f}{dt} = \mu_f P_f - m_f P_f - G_{f,mi} P_f - K P_f, \qquad (A.9)$$

$$\frac{dP_{df}}{dt} = \mu_{df} P_{df} - m_{df} P_{df} - G_{df,me} P_{df} - K P_{df}, \qquad (A.10)$$

$$\frac{dP_{eh}}{dt} = \mu_{eh} P_{eh} - m_{eh} P_{eh} - G_{eh,mi} P_{eh} - K P_{eh}, \qquad (A.11)$$

where (for example in the case of diatoms, Eq. (A.8)) m_d is the mortality rate and $G_{d,me}$ the grazing rate defined below.

A.2. Zooplankton

Following Fasham (1993), the grazing rate of, for example, mesozooplankton on diatoms is assumed to take the following form:

$$G_{d,me} = \frac{g_{d,me} p_{d,me} Z_{me} P_d}{Z_{h,me}(p_{d,me} P_d + p_{df,me} P_{df} + p_{mi,me} Z_{mi}) + p_{d,me} P_d^2 + p_{df,me} P_{df}^2 + p_{mi,me} Z_{mi}^2}, \qquad (A.12)$$

where $g_{d,me}$ is the maximum ingestion rate, $Z_{h,me}$ is the half-saturation constant for ingestion and $p_{d,me}$ is the mesozooplankton preference for diatoms. The grazing rates on other food sources are analogous. The equations for zooplankton are therefore:

$$\frac{dZ_{mi}}{dt} = (B_{f,mi} G_{f,mi} + B_{eh,mi} G_{eh,mi} + B_{d,mi} G_{d,mi}) Z_{mi}$$
$$- e_{mi} Z_{mi} - m_{mi} Z_{mi}^2 - G_{mi,me} Z_{mi}$$
$$- \frac{h(t)}{M} Z_{mi}, \qquad (A.13)$$

$$\frac{dZ_{me}}{dt} = (B_{d,me} G_{d,me} + B_{df,me} G_{df} + B_{mi,me} G_{mi}) Z_{me}$$
$$- e_{me} Z_{me} - m_{me} Z_{me}^2 - \frac{h(t)}{M} Z_{me}, \qquad (A.14)$$

$B_{f,mi}$ is, for example, the assimilation efficiency of flagellates by microzooplankton, and e_{mi} and m_{mi} are the microzooplankton excretion and mortality rates, respectively.

A.3. Nutrients

The nutrient equations are as follow:

$$\frac{dN}{dt} = - \mu_{0,d} f(T) \Psi_d(I) \Phi_d(N, A, S) \frac{n_d}{n_d + a_d} P_d$$
$$- \mu_{0,f} f(T) \Psi_f(I) n_f P_f$$
$$- \mu_{0,df} f(T) \Psi_{df}(I) n_{df} P_{df}$$
$$- \mu_{0,eh} f(T) \Psi_{eh}(I) n_{eh} P_{eh}$$
$$+ \Omega A + K(N_0 - N), \qquad (A.15)$$

$$\frac{dA}{dt} = - \mu_{0,d} f(T) \Psi_d(I) \Phi_d(N, A, S) \frac{a_d}{n_d + a_d} P_d$$
$$- \mu_{0,f} f(T) \Psi_f(I) a_f P_f$$
$$- \mu_{0,df} f(T) \Psi_{df}(I) a_{df} P_{df}$$
$$- \mu_{0,eh} f(T) \Psi_{eh}(I) a_{eh} P_{eh}$$
$$+ m_D D + (e_{mi} + \delta_{mi} m_{mi} Z_{mi}) Z_{mi}$$
$$+ (e_{me} + \delta_{me} m_{me} Z_{me}) Z_{me}$$
$$- \Omega A - KA, \qquad (A.16)$$

$$\frac{dS}{dt} = -\mu_d P_d + K(S_0 - S). \qquad (A.17)$$

The constant terms N_0 and S_0 represent the concentrations below the mixed layer depth of nitrate and silicate, respectively. Note that ammonium concentration below the MLD is assumed to be zero. The equation for ammonium (A.16) shows the balance between the loss due to ammonium uptake by phytoplankton and due to nitrification (ΩA) and gains from zooplankton excretion and detrital remineralisation (see below). A Si:N ratio of 1:1 is assumed in Eq. (A.17).

A.4. Detritus

The equation for detritus is

$$
\frac{\mathrm{d}D}{\mathrm{d}t} = (1 - B_{\mathrm{d,me}})G_{\mathrm{d,me}} + (1 - B_{\mathrm{df,me}})G_{\mathrm{df,me}}
$$
$$
+ (1 - B_{\mathrm{mi,me}})G_{\mathrm{mi,me}}
$$
$$
+ (1 - B_{\mathrm{eh,mi}})G_{\mathrm{eh,mi}}
$$
$$
+ (1 - B_{\mathrm{f,mi}})G_{\mathrm{f,mi}} + (1 - B_{\mathrm{d,mi}})G_{\mathrm{d,mi}}
$$
$$
+ m_{\mathrm{d}}P_{\mathrm{d}} + m_{\mathrm{f}}P_{\mathrm{f}} + m_{\mathrm{df}}P_{\mathrm{df}} + m_{\mathrm{eh}}P_{\mathrm{eh}}
$$
$$
- m_{\mathrm{D}}D - \left(\frac{v_{\mathrm{D}}}{M} + K\right)D, \tag{A.18}
$$

where m_{D} is the breakdown rate of detritus to ammonium. The source of detritus in the mixed layer are assumed to be dead phytoplankton and zooplankton faecal pellets.

A.5. Coccoliths

Coccoliths are represented in the model as attached (i.e. part of the coccosphere) and free coccoliths (i.e. which have become detached from the coccosphere), L_{a} and L_{f}, respectively.

The synthesis of new coccoliths is made proportional to the number of *E. huxleyi* cells and the changes in the two state variables are represented by

$$
\frac{\mathrm{d}L_{\mathrm{a}}}{\mathrm{d}t} = \rho_{\mathrm{CN}}C_{\max}f(T)\Psi(I)P_{\mathrm{eh}} - G_{\mathrm{eh,mi}}L_{\mathrm{a}}
$$
$$
- m_{\mathrm{eh}}L_{\mathrm{a}} - \Gamma - KL_{\mathrm{a}}, \tag{A.19}
$$

$$
\frac{\mathrm{d}L_{\mathrm{f}}}{\mathrm{d}t} = \Gamma + m_{\mathrm{eh}}L_{\mathrm{a}} - \delta_{\mathrm{f}}G_{\mathrm{eh,mi}}L_{\mathrm{f}} - \Theta L_{\mathrm{f}} - KL_{\mathrm{f}},
$$
$$
\tag{A.20}
$$

where ρ_{CN} is the C:N ratio and $C_{\max}$ the constant rate of calcification (i.e. coccolith production) under optimal conditions. $f(T)$ and $\Psi(I)$ represent temperature and light dependence of calcification, respectively. The transfer from attached to free coccoliths is calculated by comparing the concentration of attached coccoliths with the concentration of *E. huxleyi* cells. When the ratio of these two variables is greater than the maximum number of coccoliths allowed per cell ($\Pi_{\max}$), then all the excess coccoliths are transferred to the pool of free coccoliths. The number of coccoliths in excess is

calculated with:

$$
\Gamma = \gamma \left(L_{\mathrm{a}} - \Pi_{\max}C_{\mathrm{L}}\frac{\rho_{\mathrm{CN}}P_{\mathrm{eh}}}{C_{\mathrm{eh}}}\right). \tag{A.21}
$$

Other parameters and variables are described in Table 2.

References

Aksnes, D.L., Egge, J.K., Rosland, R., Heimdal, B.R., 1994. Representation of *Emiliania huxleyi* in phytoplankton simulation models: a first approach. Sarsia 79, 291–300.

Anonymous, 2002. Data Record of the Oceanographic Observations and Exploratory Fishing, vol. 41, 42, (part 2), 43, 44, 45, Faculty of Fisheries, Hokkaido University, Hakodate, Japan, 2002.

Anderson, T.R., 1993. A spectrally averaged model of light penetration and photosynthesis. Limnology and Oceanography 38 (7), 1403–1419.

Archer, S.D., Widdecombe, C.E., Tarran, G.A., Rees, A.P., Burkill, P.H., 2001. Production and turnover of particulate dimethylsulphonioprionate during a coccolithophore bloom in the northern North Sea. Aquatic Microbial Ecology 24, 225–241.

Baduini, C.L., Hyrenbach, K.D., Coyle, K.O., Pinchuk, A., Mendenhall, V., Hunt Jr., G.L., 2001. Mass mortality of short-tailed shearwaters in the south-eastern Bering Sea during summer 1997. Fisheries Oceanography 10 (1), 117–130.

Balch, W.M., Holligan, P.M., Kilpatrick, K.A., 1992. Calcification, photosynthesis and growth of the bloom-forming coccolithophore. *Emiliania huxleyi*. Continental Shelf Research 12, 1353–1374.

Balch, W.M., Kilpatrick, K.A., Holligan, P.M., Cucci, T., 1993. Coccolith production and detachment by *Emiliania huxleyi* (Prymnesiophyceae). Journal of Phycology 29, 566–575.

Brand, L.E., 1994. Physiological ecology of marine coccolithophores. In: Winter, A., Seisser, W.G. (Eds.), Coccolithophores. Cambridge University Press, Cambridge, pp. 39–49.

Brodeur, R.D., Sugisaki, H., Hunt Jr., G.L., 2002. Increases in jellyfish biomass in the Bering Sea: implications for the ecosystem. Marine Ecology Progress Series 233, 89–103.

Broerse, A.T.C., Tyrrell, T., Young, J.R., Poulton, A.J., Merico, A., Balch, W.M., Miller, P.I., 2003. The cause of bright waters in the Bering Sea in winter. Continental Shelf Research 23, 1579–1596.

Burkill, P.H., Mantoura, R.F.C., Llewellyn, C.A., Owens, N.J.P., 1987. Microzooplankton grazing and selectivity of phytoplankton in coastal waters. Marine Biology 93, 581–590.

Coachman, L.K., 1986. Circulation, water masses, and fluxes on the southeastern Bering Sea shelf. Continental Shelf Research 5, 23–108.

Doney, S.C., Glover, D.M., Najjar, R.G., 1996. A new coupled, one-dimensional biological-physical model for the upper

ocean: applications to the JGOFS Bermuda Atlantic time-series study BATS site. Deep-Sea Research Part II 43, 591–624.

Egge, J.K., Aksnes, D.L., 1992. Silicate as regulating nutrient in phytoplankton competition. Marine Ecology Progress Series 83, 281–289.

Eppley, R.W., 1972. Temperature and phytoplankton growth in the sea. Fishery Bullettin 70, 1063–1085.

Eslinger, D.L., Iverson, R.L., 2001. The effects of convective and wind-driven mixing on spring phytoplankton dynamics in the southeastern Bering Sea middle shelf domain. Continental Shelf Research 21, 627–650.

Evans, G.T., 1988. A framework for discussing seasonal succession and coexistence of phytoplankton species. Limnology and Oceanography 33 (5), 1027–1036.

Fasham, M.J.R., 1993. Modelling marine biota. In: Heimann, M. (Ed.), The Global Carbon Cycle. Springer, Heidelberg, pp. 457–504.

Fasham, M.J.R., 1995. Variations in the seasonal cycle of biological production in subarctic oceans: a model sensitivity analysis. Deep-Sea Research I 42 (7), 1111–1149.

Fasham, M.J.R., Ducklow, H.W., McKelvie, S.M., 1990. A nitrogen-based model of plankton dynamics in the oceanic mixed layer. Journal of Marine Research 48, 591–639.

Fernández, E., Boyd, P., Holligan, P.M., Harbour, D.S., 1993. Production of organic and inorganic carbon within a large-scale coccolithophore bloom in the northeast Atlantic Ocean. Marine Ecology Progress Series 97, 271–285.

Fileman, E.S., Cummings, D.G., Llewellyn, C.A., 2002. Microzooplankton community structure and the impact of microzooplankton grazing during an Emiliania huxleyi bloom, off the Devon coast. Journal of the Marine Biological Association of the UK 82, 359–368.

Goering, J.J., Iverson, R.L., 1981. Phytoplankton distribution on the southeastern Bering Sea shelf. In: Hood, D.W., Calder, J.A. (Eds.), The Eastern Bering Sea Shelf: Oceanography and Resources, vol. 2. University of Washington Press, Seattle, pp. 933–946.

Hansen, P.J., Calado, A.J., 1999. Phagotrophic mechanisms and prey selection in free-living dinoflagellates. Journal of Eukaryotic Microbiology 46 (4), 382–389.

Harris, R.P., 1994. Zooplankton grazing on the coccolithophore Emiliania huxleyi and its role in inorganic carbon flux. Marine Biology 119, 431–439.

Holligan, P.M., Viollier, M., Harbour, D.S., Camus, P., Champagne-Philippe, M., 1983. Satellite and ship studies of coccolithophore production along a continental shelf edge. Nature 304, 339–342.

Holligan, P.M., et al., 1993. A biogeochemical study of the coccolithophore Emiliania huxleyi in the North Atlantic. Global Biogeochemical Cycles 7 (4), 879–900.

Honjo, S., Roman, M.R., 1978. Marine copepod fecal pellets: production transportation and sedimentation. Journal of Marine Research 36, 45–57.

Hurlburt, E.M., 1990. Description of phytoplankton and nutrient in spring in the western North Atlantic Ocean. Journal of Plankton Research 12, 1–28.

Jacobson, D.M., Anderson, D.M., 1986. Thecate heterotrophic dinoflagellates: feeding behaviour and mechanisms. Journal of Phycology 22, 249–258.

Kirk, J.T.O., 1994. Light and Photosynthesis in Aquatic Ecosystems, second ed. Cambridge University Press, Cambridge.

Lessard, E.J., Murrell, M.C., 1998. Microzooplankton herbivory and phytoplankton growth in the northwestern Sargasso Sea. Aquatic Microbial Ecology 16, 173–188.

Levasseur, M., et al., 1996. Production of DMSP and DMS during a mesocosm study of an Emiliania huxleyi bloom: influence of bacteria and Calanus finmarchicus grazing. Marine Biology 126, 609–618.

Menden-Deuer, S., Lessard, E.J., 2000. Carbon to volume relationships for dinoflagellates, diatoms and other protist plankton. Limnology and Oceanography 45 (3), 569–579.

Merico, A., Tyrrell, T., Brown, C.W., Groom, S.B., Miller, P.I., 2003. Analysis of satellite imagery for Emiliania huxleyi blooms in the Bering Sea before 1997. Geophysical Research Letters 30 (6), 1337–1340.

Milliman, J.D., Troy, P.J., Balch, W.M., Adams, A.K., Li, Y.-H., Mackenzie, F.T., 1999. Biologically mediated dissolution of calcium carbonate above the chemical lysocline? Deep-Sea Research I 46, 1653–1669.

Moisan, J.R., Moisan, T.A., Abbott, M.R., 2002. Modelling the effect of temperature on the maximum growth rates of phytoplankton populations. Ecological Modelling 153, 197–215.

Nanninga, H.J., Tyrrell, T., 1996. Importance of light for the formation of algal blooms of Emiliania huxleyi. Marine Ecology Progress Series 136, 195–203.

Olson, M.B., Strom, S.L., 2002. Phytoplankton growth, microzooplankton herbivory and community structure in the southeast Bering Sea: insight into the formation and temporal persistence of an Emiliania huxleyi bloom. Deep-Sea Research II 49, 5969–5990.

Overland, J.E., Bond, N.A., Adams, J.M., 2001. North Pacific atmospheric and SST anomalies in 1997: links to ENSO? Fisheries Oceanography 10 (1), 69–80.

Paasche, E., 2002. A review of the coccolithophorid Emiliania huxleyi (Prymnesiophyceae), with particular reference to growth, coccolith formation, and calcification-photosynthesis interaction. Phycologia 40 (6), 503–529.

Platt, T., Gallegos, C.L., Harrison, W.G., 1980. Photoinhibition of photosynthesis in natural assemblages of marine phytoplankton. Journal of Marine Research 38, 687–701.

Ragueneau, O., et al., 2000. A review of the Si cycle in the modern ocean: recent progress and missing gaps in the application of biogenic opal as a paleoproductivity proxy. Global and Planetary Change 26, 317–365.

Riegman, R., Stolte, W., Noordeloos, A.A.M., Slezak, D., 2000. Nutrient uptake and alkaline phosphatase (EC 3:1:3:1) activity of Emiliania huxleyi (Prymnesiophyceae) during growth under N and P limitation in continuous cultures. Journal of Phycology 36, 87–96.

Sambroto, R.N., Niebauer, H.J., Goering, J.J., Iverson, R.L., 1986. Relationships among vertical mixing, nitrate uptake

and phytoplankton growth during the spring bloom in the southeast Bering Sea middle shelf. Continental Shelf Research 5, 161–198.

Sarmiento, J.L., Slater, R.D., Fasham, M.J.R., Ducklow, H.W., Toggweiler, J.R., Evans, G.T., 1993. A seasonal 3-dimensional ecosystem model of nitrogen cycling in the North-Atlantic euphotic zone. Global Biogeochemical Cycles 7, 450–471.

Stabeno, P.J., Bond, N.A., Kachel, N.B., Salo, S.A., Schumacher, J.D., 2001. On the temporal variability of the physical environment over the south-eastern Bering Sea. Fisheries Oceanography 10 (1), 81–98.

Stockwell, D.A., et al., 2001. Anomalous conditions in the south-eastern Bering Sea 1997: nutrients, phytoplankton and zooplankton. Fisheries Oceanography 10 (1), 99–116.

Strom, S.L., Brainard, M.A., Holmes, J.L., Olson, M.B., 2001. Phytoplankton blooms are strongly impacted by micro-zooplankton grazing in coastal North Pacific waters. Marine Biology 138, 355–368.

Strom, S., Wolfe, G., Holmes, J., Stecher, H., Shimeneck, C., Lambers, S., Moreno, E., 2003. Chemical defense in the microplankton: feeding and growth rates of heterotrophic protists on the DMS-producing phytoplankter *Emiliania huxleyi*. Limnology and Oceanography 48, 217–229.

Sukhanova, I.N., Flint, M.V., 1998. Anomalous blooming of coccolithophorids over the eastern Bering Sea shelf. Oceanology 38 (4), 502–505.

Sukhanova, I.N., Semina, H.J., Venttsel, M.V., 1999. Spatial distribution and temporal variability of phytoplankton in the Bering Sea. In: Loughlin, T.R., Ohtani, K. (Eds.), Dynamics of the Bering Sea. University of Alaska Sea Grant, Fairbanks, pp. 453–483.

Taniguchi, A., Saito, K., Koyama, A., 1976. Phytoplankton communities in the Bering Sea and adjacent seas. Journal of the Oceanographical Society of Japan 32, 99–106.

Tyrrell, T., Taylor, A.H., 1996. A modelling study of *Emiliania huxleyi* in the NE Atlantic. Journal of Marine System 9, 83–112.

Tyrrell, T., Holligan, P.M., Mobley, C.D., 1999. Optical impacts of oceanic coccolithophore blooms. Journal of Geophysical Research 104 (C2), 3223–3241.

Vance, T.C., et al., 1998. Aquamarine waters recorded for first time in eastern Bering Sea. EOS Transactions of the American Geophysical Union 79 (10), 121–126.

Verity, P.G., Smetacek, V., 1996. Organism life cycles, predation, and the structure of marine pelagic ecosystems. Marine Ecology Progress Series 130, 277–293.

Walsh, J.J., et al., 1989. Carbon and nitrogen cycling with the Bering/Chukchi Seas: Sources regions for organic matter affecting AOU demands of the Arctic Ocean. Progress in Oceanography 22, 277–359.

Westbroek, P., et al., 1993. A model system approach to biological climate forcing: the example of *Emiliania huxleyi*. Global Planetary Change 8, 27–46.

Winter, A., Jordan, R.W., Roth, P.H., 1994. Biogeography of living coccolithophores in ocean waters. In: Winter, A., Siesser, W.G. (Eds.), Coccolithophores. Cambridge University Press, Cambridge, pp. 39–49.

Young, J.R., 1994. Functions of coccoliths. In: Winter, A., Siesser, W.G. (Eds.), Coccolithophores. Cambridge University Press, Cambridge, pp. 63–82.